Ultrasound in Med. & Biol., Vol. 44, No. 11, pp. 2241–2249, 2018

0301-5629/$ - see front matter

https://doi.org/10.1016/j.ultrasmedbio.2018.06.006

● *Original Contribution*

NON-INVASIVE CHARACTERIZATION OF FOCAL ARRHYTHMIA WITH ELECTROMECHANICAL WAVE IMAGING *IN VIVO*

Alexandre Costet,* Elaine Wan,† Lea Melki,* Ethan Bunting,* Julien Grondin,* Hasan Garan,† and Elisa Konofagou*,‡

* Department of Biomedical Engineering, Columbia University, New York, New York, USA; † Department of Medicine—Cardiology, Columbia University, New York, New York, USA; and ‡ Department of Radiology, Columbia University, New York, New York, USA

(*Received* 18 *November* 2017; *revised* 5 *June* 2018; *in final from* 11 *June* 2018)

Abstract—There is currently no established method for the non-invasive characterization of arrhythmia and differentiation between endocardial and epicardial triggers at the point of care. Electromechanical wave imaging (EWI) is a novel ultrasound-based imaging technique based on time-domain transient strain estimation that can map and characterize electromechanical activation in the heart *in vivo*. The objectives of this initial feasibility study were to determine that EWI is capable of differentiating between endocardial and epicardial sources of focal rhythm and, as a proof-of-concept, that EWI could characterize focal arrhythmia in one patient with premature ventricular contractions (PVCs) before radiofrequency (RF) ablation treatment. First, validation of EWI for differentiation of surface of origin was performed in seven (n = 7) adult dogs using four epicardial and four endocardial pacing protocols. Second, one (n = 1) adult patient diagnosed with PVC was imaged with EWI before the scheduled RF ablation procedure, and EWI results were compared with mapping procedure results. In dogs, EWI was capable of detecting whether pacing was of endocardial or epicardial origin in six of seven cases (86% success rate). In the PVC patient, EWI correctly identified both regions and surface of origin, as confirmed by results from the electrical mapping obtained from the RF ablation procedure. These results reveal that EWI can map the electromechanical activation across the myocardium and indicate that EWI could serve as a valuable pre-treatment planning tool in the clinic. (E-mail: ek2191@columbia.edu)

Key Words: **Arrhythmias, Electromechanical activation, Electromechanical wave imaging, Non-invasive imaging, Premature ventricular contraction, Strain, Ultrasound.**

INTRODUCTION

Sources of focal ventricular arrhythmia may be located in the left or right ventricle, on the endocardium, in mid-myocardium or on the epicardium (Kaltenbrunner et al. 1991). For example, the prevalence of epicardial focal ventricular tachycardia (VT) is around 7%–13% of all focal VTs (Sacher et al. 2008; Tada et al. 2001). Radiofrequency (RF) catheter ablation for the treatment of VT, introduced in the early 1980s, has become one of the main options available to treat VT, and successful ablation hinges on correctly determining the site of origin of the arrhythmia (Njeim and Bogun 2015). The 12-lead electrocardiogram (ECG) is used for initial diagnostics and may reveal characteristics that enable physicians to infer the location of the origin, although the criteria seem to be limited (Bazan et al. 2007; Berruezo et al. 2004). The methods most commonly used to determine the origin of an arrhythmia are invasive catheterization techniques, such as activation sequence mapping and pace mapping (Moreno et al. 2005; Nademanee and Kosar 1998). Endocardial and epicardial mapping approaches differ, and because there is currently no non-invasive imaging technique capable of differentiating between endocardial and epicardial origin, an ablation procedure often consists of an electrophysiology study during which endocardial catheter mapping is performed and which may be followed by epicardial catheter mapping when endocardial mapping fails to identify an origin (Sosa et al. 1998).

Electromechanical wave imaging (EWI) is a non-invasive, non-ionizing, ultrasound-based imaging modality that can map the electromechanical activity of the heart in all four chambers at high spatial and

Address correspondence to: Elisa Konofagou, 1210 Amsterdam Avenue, ET351, MC 8904, New York, NY, 10027. E-mail: ek2191@columbia.edu

temporal resolution, with real-time feedback capabilities (Costet et al. 2014; Konofagou et al. 2010; Provost et al. 2010, 2011a, 2011b, 2013). At the tissue level, the depolarization of the myocardium triggers the electromechanical activation, that is, the first time at which the muscle transitions from a relaxation to a contraction state, and the spatial propagation of the electromechanical activation forms the electromechanical wave (EW) that follows the pattern of propagation of the electrical activation sequence. Unlike tissue Doppler methods, which rely on the use of frequency domain technique to estimate velocity and strain (Koyama et al. 2003; Uematsu et al. 1995), EWI relies on speckle-tracking techniques to estimate minute displacements and incremental (or inter-frame) strains in the time domain at a sufficiently high frame rate to enable tracking the EW through systole.

Electromechanical activation times rely on the onset of the mechanical activation and are essentially a surrogate for the electrical activation. Indeed, previous studies have found that EW propagation is highly correlated with the underlying electrical activation in all four chambers of the heart in normal canine hearts during sinus rhythm and various pacing protocols *in vivo* and *in silico* (Costet et al. 2016; Provost et al. 2011a, 2011b). Additionally, EWI has been reported to be capable of mapping the electromechanical activation sequence in both human (Provost et al. 2013, 2015) and canine (Costet et al. 2014, 2015; Provost et al. 2010, 2011a, 2011b) models, during sinus rhythm, pacing and both focal and re-entrant arrhythmias. EWI is not limited to the endocardial or epicardial surface and is capable of mapping the EW transmurally, but whether EWI is capable of differentiating between endocardial and epicardial origins has not yet been determined. If EWI had the potential not only to identify the region of the heart responsible for a focal ventricular arrhythmia, but also to distinguish between endocardial and epicardial origins, it would be a particularly useful clinical tool for planning treatment with RF catheter ablation as it could eliminate unnecessary endocardial mapping when the origin of the arrhythmia is located at the epicardial level.

We hypothesized that EWI is capable of differentiating between endocardial and epicardial sources of focal arrhythmia and that it could be used to plan intracardiac mapping and RF ablation procedures. To test this hypothesis, we first aimed to illustrate that EWI is capable of differentiating between endocardial and epicardial sources of focal rhythm, and second, we presented a proof-of-concept that EWI is capable of characterizing focal arrhythmia and predicting its origin noninvasively before mapping and ablation. To reach that goal, we first performed a feasibility study in a paced animal model in which we attempted to simulate focal ventricular arrhythmia by pacing the hearts of adult mongrel dogs from the epicardium and the endocardium. Then, we acquired EWI in one patient diagnosed with premature ventricular contraction (PVC) before their scheduled mapping and RF ablation procedures. PVCs are additional, abnormal heartbeats originating in either ventricle that can be treated by ablating the region from which they originate. Pseudo-3-D maps of the PVC patient's electromechanical activation, as well as videos of the activation, were generated. These were used to determine that EWI is capable of identifying the earliest region of activation and correctly differentiating between endocardial and epicardial foci, and, as a proof-of-concept in one patient, EWI results were compared with the findings of the electrophysiology mapping procedures to confirm the accuracy of the prediction.

METHODS

Experimental animal protocol

This study complied with the Public Health Service Policy on Humane Care and Use of Laboratory Animals and was approved by the Institutional Animal Care and Use Committee of Columbia University. Seven adult mongrel dogs (N = 7) were used in this study. After lateral thoracotomy, the pericardium was removed, and a pericardial cradle was formed to exclude the lungs and support the heart to expose the apex. Epicardial pacing was performed in four animals (n = 4). A bipolar electrode of an ablation catheter (TactiCath, St. Jude Medical, Secaucus, NJ, USA) was used in two dogs (n = 2) for epicardial pacing by manually placing the electrode at the mid-level, slightly toward the apex. In two other dogs, epicardial pacing was performed through pacing electrodes sutured to the lateral wall near the base (n = 1) or to the posterior-lateral wall at the mid-level (n = 1). Endocardial pacing was performed on four animals (n = 4) by placing a 64-electrode basket catheter (Constellation, Boston Scientific, Natick, MA, USA) in the left ventricle (LV) and pacing using two of its adjacent electrodes. For endocardial pacing with the basket catheter, we chose electrodes located at the mid-level providing good contact with the endocardium. Please note that of the 7 animals, 1 was used for both epicardial and endocardial pacing. The pacing rate was chosen just high enough to overdrive the intrinsic sinus rhythm, and the voltage output was set at 10 V. For this validation study, EWI acquisition was performed open chest by placing the probe coated with ultrasound gel directly at the apex. Pacing locations are summarized in Table 1. EWI was acquired while pacing open-chest canines in the standard apical echocardiographic views (4-, 2- and 3-chamber), with the addition of a view taken in between

Table 1. Summary of pacing locations for the paced animal model

Dog	Pacing site	Location	Pacing rate (ms)	Pacing voltage (V)
1	Epicardial	Anterior-lateral	400	10
2	Epicardial	Anterior-lateral	550	10
3	Epicardial	Lateral	400	10
4	Epicardial	Posterior-lateral	500	10
1	Endocardial	Posterior-lateral	400	10
5	Endocardial	Anterior-lateral	600	10
6	Endocardial	Anterior	500	10
7	Endocardial	Posterior	500	10

the 2- and 4-chamber views that we call "3.5-chamber" view.

Clinical study protocol and patient selection

The clinical study protocol was approved by the institutional review board (Protocol AAAA9333) of Columbia University, and written informed consent was obtained from the patient before scanning. One 70-year-old patient diagnosed with PVC underwent EWI scanning by a trained cardiologist a few minutes before an electro-anatomic mapping and ablation procedure. The ablation procedure was successful and mapping results were obtained and compared with EWI findings for validation. Non-invasive EWI acquisition was performed transthoracically in the standard apical echocardiographic views (4-, 2- and 3-chamber) with the addition of the 3.5-chamber view as previously described. EWI was acquired during pre-excitation as seen on the electrocardiogram (ECG).

Electromechanical wave imaging

Acquired data were processed as previously described elsewhere (Costet et al. 2014; Grondin et al. 2016; Provost et al. 2011b, 2013). Briefly, an unfocused transmit sequence was implemented on a Verasonics system (Verasonics, Redmond, WA, USA) to acquire frames at 2000 fps using a 2.5-MHz ATL P4-2 phased array (Fig. 1.1) (Provost et al. 2011b). Beamforming on the signals obtained from each of the elements was performed during post-processing, resulting in the reconstruction of one RF frame per transmit. RF frames denote the beamformed, unprocessed and unfiltered ultrasound images and contain phase information that is lost when generating B-mode images. The reconstructed images had an angular sampling of 0.7° or 0.025 rad (128 lines spanning 90°) and an axial sampling frequency of 20 MHz (axial sampling of 0.0385 mm) (Fig. 1.2). Segmentation of the LV myocardium was manually performed on the first frame of the anatomic B-mode sequence, and the myocardial contour was subsequently automatically tracked throughout the cardiac cycle using the estimated displacements (Luo and Konofagou 2008). Displacement estimation was performed in MATLAB (The MathWorks, Natick, MA, USA) using a fast, 1-D RF-based cross-correlation algorithm because it has been reported that RF-based speckle tracking offers far greater accuracy than B-mode speckle tracking (Luo and Konofagou 2010; Walker and Trahey 1994). Axial incremental strains (*i.e.,* the inter-frame strain in the axial direction) were estimated using a least-squares estimator with a 5-mm, 1-D kernel (Fig. 1.3) (Kallel and Ophir 1997). Electromechanical activation was defined as the time at which the incremental strain value changes from positive (lengthening in the axial direction) to negative (shortening or contraction in the axial direction), *i.e.,* the first time point at which the incremental strain curve crosses zero after the Q-wave as seen on the ECG (Fig. 1.4). Isochrones were generated by manual selection of the first occurrence of the incremental strain zero crossing (transition from positive (relaxation) to negative (contraction) strain, *i.e.,* onset of contraction) in the LV after onset of the QRS for up to 100 automatically selected points within the segmented wall. Subsample resolution of the zero crossings was obtained through cubic spline interpolation. Smooth continuous isochronal maps were then generated through Delaunay triangulation-based cubic interpolation (Provost et al. 2010). All views were co-registered in Amira 5.3.3 (Visage Imaging, Chelmsford, MA, USA), both temporally (using ECG) and spatially (using B-mode anatomic landmarks such as the position of the valves and apex), to construct a pseudo-3-D isochrone (Fig. 1.5). The color bar ranges from red for earliest activation timings to black for the latest activation timings. Finally, videos of the electromechanical activation propagation were generated from the electromechanical activation times.

RESULTS

Animal study: Endocardial versus epicardial pacing origin

Figures 2 and 3 depict the results of EWI during endocardial and epicardial pacing, respectively. The pseudo-3-D isochrones of the electromechanical activation are presented for each pacing location, and a magnified region of interest (ROI) selected manually and revealing details of the earliest region of activation is depicted as well.

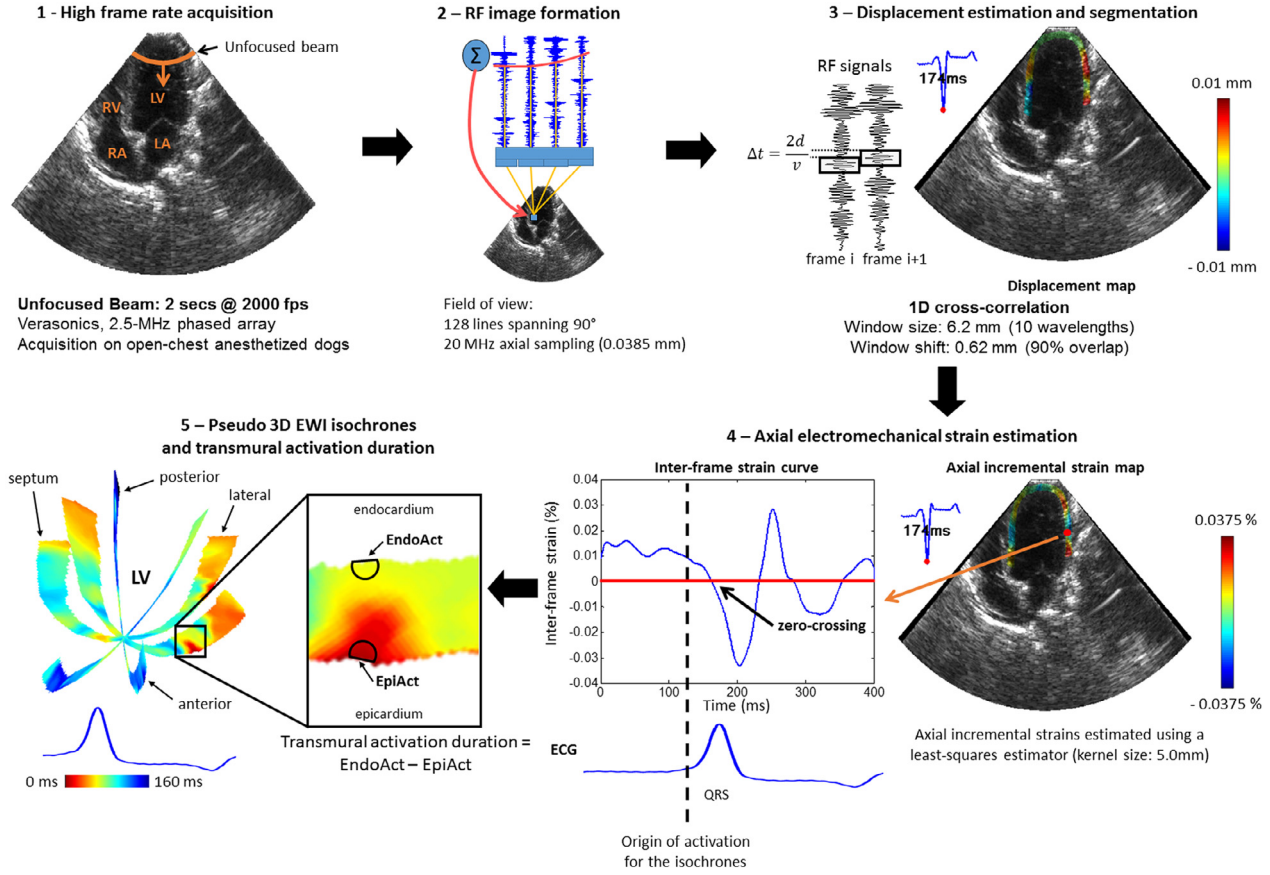

Fig. 1. Flowchart of EWI acquisition and motion and strain estimation flowchart. (1) Two seconds of high-frame-rate acquisition (2000 Hz) in standard apical views with an unfocused transmit sequence. (2) RF image formation using channel data. (3) Segmentation and 1-D axial displacement estimation using 1-D cross-correlation. (4) Axial incremental strain estimated using a least-squares estimator. (5) EWI isochrones for each apical view are obtained by selecting the zero crossings within the mask, and pseudo-3-D isochrones are generated. ECG = electrocardiography; EWI = electromechanical wave imaging; LV = left ventricle; RF = radiofrequency.

Figure 2 and Supplementary Video S1 (online only) depict the results obtained during epicardial pacing. Locations of pacing included the LV anterior-lateral wall (Fig. 2A, B), the LV basal lateral wall (Fig. 2C) and the LV posterior-lateral wall (Fig. 2D). In all four animals, the origin of the electromechanical activation was correctly detected at the location of pacing. During epicardial pacing in dog 1 (Fig. 2A), the earliest region of electromechanical activation was detected on the anterior-lateral wall at the mid-level. The magnified ROI clearly reveals that the activation started in the epicardium and propagated to the endocardium. During epicardial pacing in dog 2 (Fig. 2B), the earliest region of electromechanical activation was also detected epicardially on the anterior-lateral wall, near the apex. Early activation observed epicardially on the lateral wall suggests that the electromechanical activation propagated along the epicardial wall toward the lateral wall. The magnified ROI reveals early epicardial activation followed by propagation toward the base (to the right of the magnified ROI). During epicardial pacing in dog 3 (Fig. 2C), the earliest activated region was detected on the lateral wall on the epicardium, near the base. The electromechanical activation propagated from the epicardium down toward the apex and the endocardium, as can also be seen in the magnified ROI. In dog 6, EWI was not capable of revealing the early activation originating from the epicardium and propagating to the endocardium, although it correctly detected the earliest region of activation on the posterior-lateral wall (Fig. 2D). Video of the activation for dogs 1, 2 and 3 (Supplementary Video S1) clearly depicts the electromechanical activation originating epicardially and propagating toward the endocardium.

In Figure 3 are the results obtained during endocardial pacing. Locations of pacing included the LV posterior-lateral wall (Fig. 3A), the LV anterior-lateral wall (Fig. 3B), the LV anterior wall (Fig. 3C) and the LV

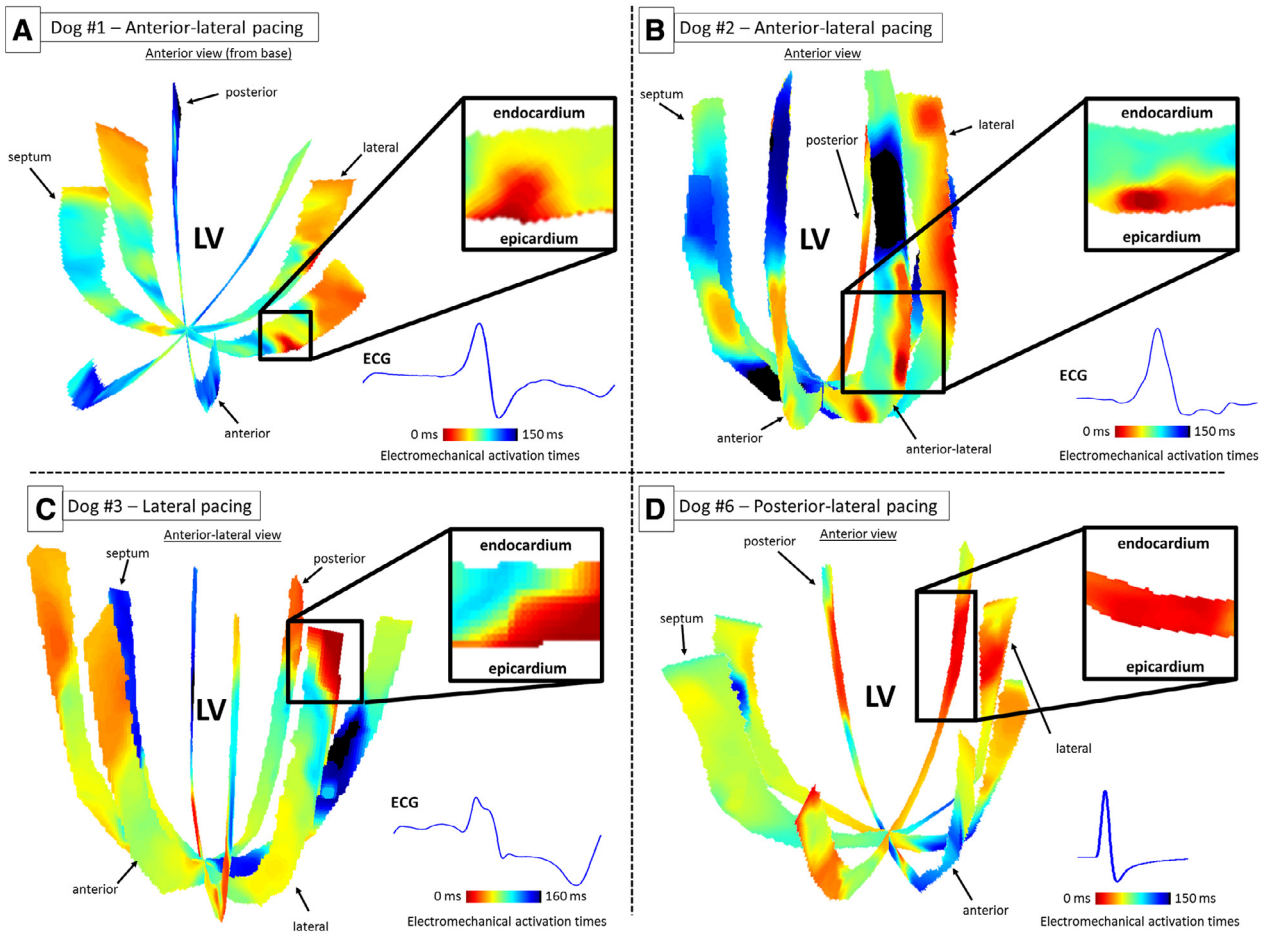

Fig. 2. EWI results from epicardial pacing. Pseudo-3-D isochrones indicate the location of the earliest region of activation. Magnified regions of interest indicate the earliest region of activation. (A–C) Activation originated from the epicardium and propagated toward the endocardium. (D) The earliest region of activation corresponded to the location of pacing, but the surface of origin was not distinguishable. ECG = electrocardiography; EndoAct = endocardial activation; EpiAct = epicardial activation; LV = left ventricle.

posterior wall (Fig. 3D). In all four animals, the origin of the electromechanical activation was correctly detected at the location of pacing. During endocardial pacing in dog 1 (Fig. 3A), the earliest electromechanical activation was detected in the posterior-lateral wall at the mid-level. The magnified ROI reveals the activation originating at the endocardium and propagating toward the epicardium. During endocardial pacing in dog 5 (Fig. 3B), regions activated the earliest were detected on the lateral and anterior-lateral walls. The magnified ROI at the region of earliest activation on the lateral wall indicates that the activation started sub-endocardially and subsequently propagated toward the epicardium. During endocardial pacing in dog 6 (Fig. 3C), the electromechanical activation originated on the anterior wall at the midway between base and apex. The magnified ROI reveals details of the activation on the anterior wall endocardium propagating toward the epicardium. Finally, during posterior pacing in dog 7 (Fig. 3D), EWI was not capable of detecting the earliest activation starting from the endocardium, although it correctly identified the earliest region of activation as being located posteriorly. Video of the activation for dogs 1, 5 and 6 (Supplementary Video S2, online only) depicts that the electromechanical activation originated endocardially and propagated toward the epicardium.

Clinical proof-of-concept: PVC patient

Figure 4 depicts the results obtained from EWI acquisition in one PVC patient scheduled for ablation. Pseudo 3-D EWI isochrones are presented on the left, and electrophysiology results obtained after the mapping and ablation procedure are presented on the right. EWI isochrones for this patient depict the earliest activated region posteriorly in the right ventricle (RV). Early activation can also be posteriorly seen in the LV, which

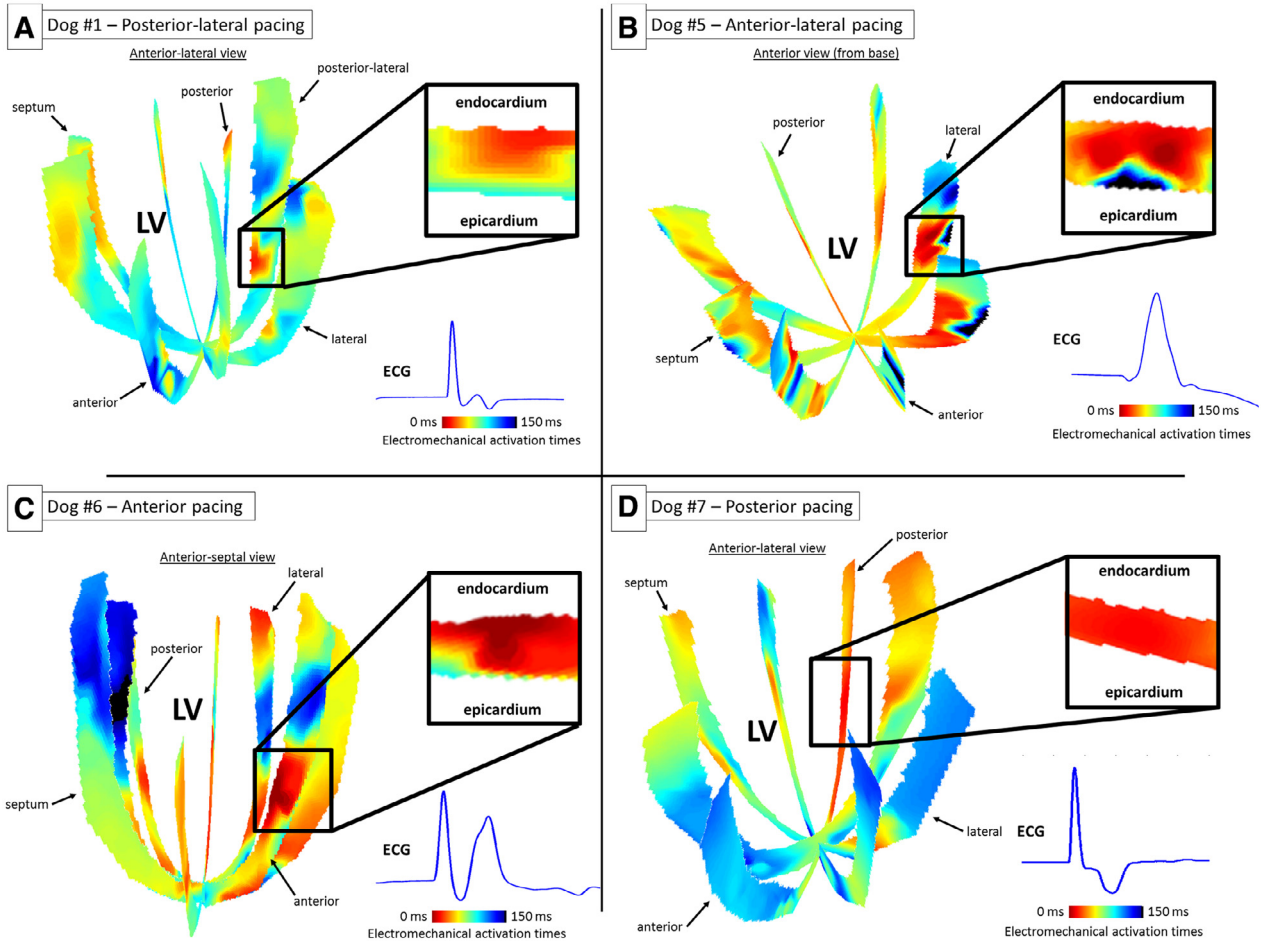

Fig. 3. Electromechanical wave imaging results from focal endocardial pacing. Pseudo-3-D isochrones indicate the location of the earliest region of activation. Magnified regions of interest indicate the earliest region of activation. (A–C) Activation originated from the endocardium and propagated toward the epicardium. (D) The earliest region of activation corresponded to the location of pacing, but the surface of origin was not distinguishable.

leads us to postulate that the PVC originates from the RV outflow tract (RVOT). Electrophysiology mapping results indicate that the PVC origin was located in the low posterior RVOT, as can been seen on the activation map in Figure 4. Ablation at this location terminated PVC activity in the patient.

DISCUSSION

The goal of this study was to verify our hypothesis that EWI is capable of differentiating between endocardial and epicardial sources of focal arrhythmia and that it could be used to plan RF ablation procedures. The hypothesis was tested using an animal model in which we could induce a focal arrhythmia and control its location and surface of origin. We also assessed whether EWI could be used to plan RF ablation by acquiring data in a patient diagnosed with PVCs and scheduled for an RF ablation, comparing EWI results with the findings of the electromechanical mapping performed during the procedure. More precisely, we assessed the potential role of EWI in characterizing focal arrhythmia by illustrating that EWI is capable not only of detecting the origin of the arrhythmia, but also of discriminating between surfaces of origin, using ventricular pacing as a surrogate rhythm for focal ventricular arrhythmia. The isochrones and videos of the electromechanical activation during pacing from endocardial and epicardial sites revealed that EWI correctly detected the origin of the electromechanical activation, that is, the onset of deformation after electrical activation, at the location of pacing. Furthermore, in six of seven cases, EWI was capable of discriminating between epicardial and endocardial pacing by depicting the earliest region of electromechanical activation as being located on either the epicardial (Fig. 2) or the endocardial (Fig. 3) surface, in accordance with the

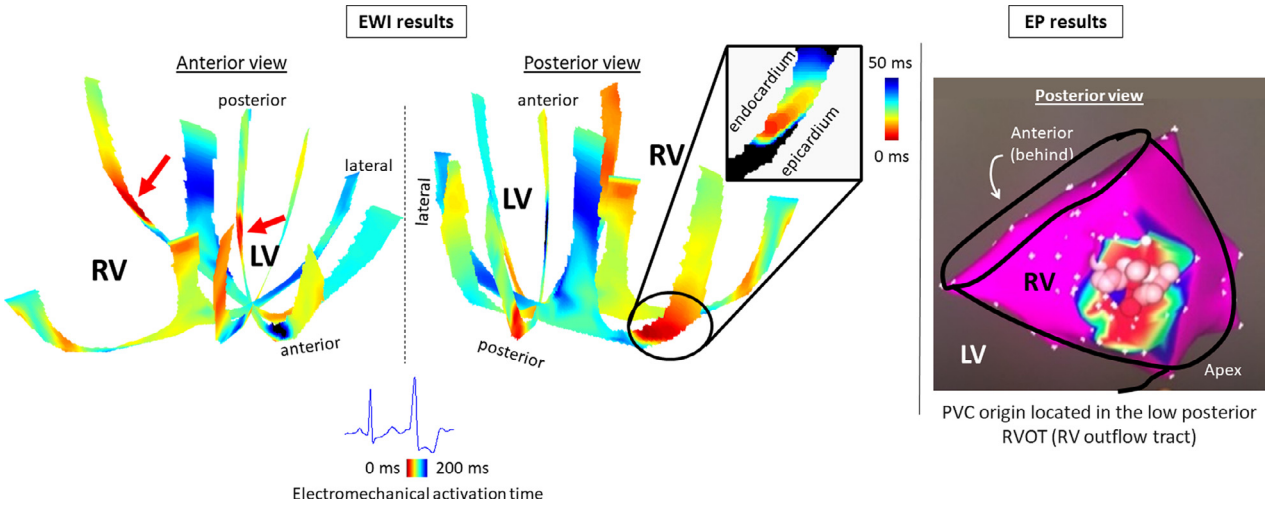

Fig. 4. Electromechanical wave imaging results in one patient scheduled for premature ventricular contraction ablation. The location of the earliest region of activation on the EWI isochrone (on the left) corresponded to the origin found during electrophysiology studies (on the right). *Red arrows* indicate region of early activation. EP = electrophysiology; EWI = electromechanical wave imaging; LV = left ventricle; PVC = premature ventricular contraction; RV = right ventricle.

site of pacing. These results confirm previous findings by our group that EWI is capable of correctly detecting the pacing origin from multiple locations in both the LV and RV (Costet et al. 2014; Provost et al. 2011a, 2011b, 2013) and extend prior capabilities by defining a novel role for EWI in determining the transmurality of rhythm initiation. Second, a clinical proof-of-concept in one patient diagnosed with PVC and scheduled for RF ablation was presented. The goal was to determine whether EWI was capable of identifying the site of origin of PVC and to confirm that location with electrophysiological mapping. We found that EWI correctly detected the region of origin in a blinded comparison, as confirmed during the mapping procedure, and that ablation of the target resulted in acute termination of the arrhythmia.

During electrophysiological procedures for the treatment of ventricular conditions such as PVC-induced VT, mapping of the arrhythmia is essential to target the adequate region to ablate. One of the shortcomings of intracardiac mapping is that it prolongs the procedure time, sometimes by a couple of hours, which may increase risks to the patient. Pre-procedure, non-invasive mapping to determine the origin of the arrhythmia is thus of great interest to physicians. Previous efforts include solving an inverse problem using body surface potential to reconstruct the epicardial activation sequence (Erkapic et al. 2015; Jamil-Copley et al. 2014; Ramanathan et al. 2004). Although the newest techniques show a lot of promise, they still require that computed tomography or magnetic resonance imaging acquisition be performed and that the patient wear a 256-electrode vest, which can be contraindicated for some. Several algorithms using 12-lead ECG acquisitions to guide ablation have also been developed (Bazan et al. 2007; Betensky et al. 2011; Ouyang et al. 2002; Vallès et al. 2010). Although non-invasive, these algorithms are region-dependent and often involve numerous steps and measurements to reach a diagnosis, which increases the probability of error and variability in the results. As a non-invasive, ultrasound-based imaging modality, we presented a proof-of-concept in which EWI was capable of providing relevant insights into the origins of an arrhythmia. This together with previous findings (Provost et al. 2011b, 2015) indicate that EWI could have the potential to position itself in the clinic as a uniquely valuable pre-procedure planning tool for the non-invasive characterization of focal arrhythmias.

Limitations include the small number of subjects involved in this study. To further confirm EWI capability in discriminating between epicardial and endocardial sources and to confirm EWI's value as a pre-treatment planning tool, an increase in the number of patients is required. Technical limitations of EWI include 2-D acquisition of apical views of the heart. Indeed, the focal arrhythmia origin might not be exactly situated in the same views as those used during EWI acquisition. This limitation is mitigated by acquiring numerous views that are then co-registered in space and time. Thus, when the focal source is located between acquisition planes, the immediately neighboring walls may both show an early activated region, which may as a result facilitate localization of the source (see, *e.g.,* Figs. 2B and 3B). However, this fails in some cases, and although EWI can provide insight into the region of origin, it is not capable

of determining the surface of origin during pacing (Figs. 2D and 3D). Additionally, misregistration of 2-D views may lead to incorrect localization of the origin; for example, EWI may locate an origin on the anterior wall when it is in fact on the anterior-lateral wall. Despite some uncertainty in pinpointing the exact location of the arrhythmic origin, EWI may still be of value to clinicians and help them plan for the mapping and ablation procedure. For example, determining if an arrhythmia originates from the left or right atrium may help clinicians plan for the potential need for a transeptal puncture. Of course, true 3-D EWI (Grondin et al. 2017) may help mitigate this issue. EWI currently relies on 1-D displacement and strain estimation, which may result in false positives that may appear as early activated regions far from the pacing location or focal arrhythmia foci. This may be due to errors in the displacement and strain estimations caused by a poor acoustic window or the misalignment between the myocardium fibers and the direction of estimation. True 3-D EWI may help to limit false positives by offering a more accurate displacement and strain estimation and is currently being investigated in our lab. Another limitation of this study could arise from the fact that the pseudo-3-D electromechanical activation isochrones are generated from four consecutive but separate acquisitions. This was not deemed as a concern in this study, however, because EWI was acquired in the case of highly organized, stable rhythms and because we had previously found EWI to be reproducible and repeatable between heart cycles both within the same acquisition and between separate acquisitions and views (Costet et al. 2014; Provost et al. 2013). Finally, in its current implementation, the total EWI acquisition time for all four views ranged from 2 to 10 min per subject, and data processing was performed offline. Although the processing time to generate pseudo-3-D maps and activation videos was no more than an hour per subject, EWI will require online implementation to truly be clinic ready, which is currently underway by our group.

CONCLUSION

EWI was demonstrated to be capable of accurately localizing the source of focal pacing in an animal model and a PVC human subject. EWI was also found to be capable of discriminating between epicardial and endocardial origins in 86% of the animals studied. We also presented proof-of-concept in which EWI was capable of non-invasively identifying the location and surface of origin of PVCs in a human subject as confirmed by electrophysiology mapping. EWI is a non-invasive, non-ionizing, ultrasound-based imaging modality that has real-time capabilities and is easily translatable to existing clinical ultrasound systems. As a result, EWI has the potential to position itself in the clinic as a valuable pre-procedure planning tool for the non-invasive characterization of focal arrhythmias.

Acknowledgments—This work was supported in part by the National Institutes of Health (R01 EB006042, R01 HL114358) and with ‘Gerstner scholarship (EW) and Esther Aboodi endowment (EW).

SUPPLEMENTARY DATA

Supplementary data related to this article can be found at doi:10.1016/j.ultrasmedbio.2018.06.006.

REFERENCES

Bazan V, Gerstenfeld EP, Garcia FC, Bala R, Rivas N, Dixit S, Zado E, Callans DJ, Marchlinski FE. Site-specific twelve-lead ECG features to identify an epicardial origin for left ventricular tachycardia in the absence of myocardial infarction. Heart Rhythm 2007;4:1403–1410.

Berruezo A, Mont L, Nava S, Chueca E, Bartholomay E, Brugada J. Electrocardiographic recognition of the epicardial origin of ventricular tachycardias. Circulation 2004;109:1842–1847.

Betensky BP, Park RE, Marchlinski FE, Hutchinson MD, Garcia FC, Dixit S, Callans DJ, Cooper JM, Bala R, Lin D, Riley MP, Gerstenfeld EP. The V2 transition ratio: A new electrocardiographic criterion for distinguishing left from right ventricular outflow tract tachycardia origin. J Am Coll Cardiol 2011;57:2255–2262.

Costet A, Provost J, Gambhir A, Bobkov Y, Danilo Jr P, Boink GJJ, Rosen MR. Konofagou EE. Electromechanical wave imaging of biologically and electrically paced canine hearts in vivo. Ultrasound Med Biol 2014;40:177–187.

Costet A, Bunting E, Grondin J, Gambhir A, Konofagou EE. Atrial electromechanical cycle length mapping in paced canine hearts in vivo. IEEE Trans Ultrason Ferroelectr Freq Control 2015;62:1277–1287.

Costet A, Wan E, Bunting E, Grondin J, Garan H, Konofagou E. Electromechanical wave imaging (EWI) validation in all four cardiac chambers with 3 D electroanatomic mapping in canines in vivo. Phys Med Biol 2016;61:8105.

Erkapic D, Greiss H, Pajitnev D, Zaltsberg S, Deubner N, Berkowitsch A, Möllman S, Sperzel J, Rolf A, Schmitt J, Hamm CW, Kuniss M, Neumann T. Clinical impact of a novel three-dimensional electrocardiographic imaging for non-invasive mapping of ventricular arrhythmias—A prospective randomized trial. Europace 2015;17:591–597.

Grondin J, Costet A, Bunting E, Gambhir A, Garan H, Wan E, Konofagou EE. Validation of electromechanical wave imaging in a canine model during pacing and sinus rhythm. Heart Rhythm 2016;13:2221–2227.

Grondin JL, Wang D, Trayanova N, Konofagou EE. 38th Heart Rhythm Society Annual Scientific Sessions (Chicago IL), May 10 to 14, 2017.

Jamil-Copley S, Bokan R, Kojodjojo P, Qureshi N, Koa-Wing M, Hayat S, Kyriacou A, Sandler B, Sohaib A, Wright I, Davies DW, Whinnett Z, S.Peters N, Kanagaratnam P, Lim PB. Noninvasive electrocardiographic mapping to guide ablation of outflow tract ventricular arrhythmias. Heart Rhythm 2014;11:587–594.

Kallel F, Ophir J. A least-squares strain estimator for elastography. Ultrason Imaging 1997;19:195–208.

Kaltenbrunner W, Cardinal R, Dubuc M, Shenasa M, Nadeau R, Tremblay G, Vermeulen M, Savard P, Pagé PL. Epicardial and endocardial mapping of ventricular tachycardia in patients with myocardial infarction: Is the origin of the tachycardia always subendocardially localized?. Circulation 1991;84:1058–1071.

Konofagou EE, Luo J, Saluja D, Cervantes DO, Coromilas J, Fujikura K. Noninvasive electromechanical wave imaging and conduction-relevant velocity estimation in vivo. Ultrasonics 2010;50:208–215.

Koyama J, Ray-Sequin PA, Falk RH. Longitudinal myocardial function assessed by tissue velocity, strain, and strain rate tissue doppler echocardiography in patients with Al (primary) cardiac amyloidosis. Circulation 2003;107:2446–2452.

Luo J, Konofagou EE. High-frame rate, full-view myocardial elastography with automated contour tracking in murine left ventricles in vivo. IEEE Trans Ultrason Ferroelectr Freq Control 2008;55:240–248.

Luo J, Konofagou E. A fast normalized cross-correlation calculation method for motion estimation. IEEE Trans Ultrason Ferroelectr Freq Control 2010;57:1347–1357.

Moreno M, Perez-Castellano N, Villacastin J. Pacemapping. Indian Pacing Electrophysiol J 2005;5:35–42.

Nademanee K, Kosar EM. A nonfluoroscopic catheter-based mapping technique to ablate focal ventricular tachycardia. Pacing Clin Electrophysiol 1998;21:1442–1447.

Njeim M, Bogun F. Selecting the appropriate ablation strategy: The role of endocardial and/or epicardial access. Arrhythm Electrophysiol Rev 2015;4:184–188.

Ouyang F, Fotuhi P, Ho SY, Hebe J, Volkmer M, Goya M, Burns M, Antz M, Ernst S, Cappato R, Kuck KH. Repetitive monomorphic ventricular tachycardia originating from the aortic sinus cusp: Electrocardiographic characterization for guiding catheter ablation. J Am Coll Cardiol 2002;39:500–508.

Provost J, Lee WN, Fujikura K, Konofagou EE. Electromechanical wave imaging of normal and ischemic hearts in vivo. IEEE Trans Med Imaging 2010;29:625–635.

Provost J, Lee WN, Fujikura K, Konofagou EE. Imaging the electromechanical activity of the heart in vivo. Proc Natl Acad Sci USA 2011;108:8565–8570.

Provost J, Nguyen VTH, Legrand D, Okrasinski SJ, Costet A, Gambhir A, Garan H, Konofagou EE. Electromechanical wave imaging for arrhythmias. Phys Med Biol 2011;56:1–11.

Provost J, Gambhir A, Vest J, Garan H, Konofagou EE. A clinical feasibility study of atrial and ventricular electromechanical wave imaging. Heart Rhythm 2013;10:856–862.

Provost J, Costet A, Wan E, Gambhir A, Whang W, Garan H, Konofagou EE. Assessing the atrial electromechanical coupling during atrial focal tachycardia, flutter, and fibrillation using electromechanical wave imaging in humans. Comput Biol Med 2015;65:161–167.

Ramanathan C, Ghanem RN, Jia P, Ryu K, Rudy Y. Noninvasive electrocardiographic imaging for cardiac electrophysiology and arrhythmia. Nature medicine 2004;10:422–428.

Sacher F, Tedrow UB, Field ME, Raymond JM, Koplan BA, Epstein LM, Stevenson WG. Ventricular tachycardia ablation evolution of patients and procedures over 8 years. Circ Arrhythm Electrophysiol 2008;1:153–161.

Sosa E, Scanavacca M, D'avila A, Piccioni J, Sanchez O, Velarde JL, Silva M, Reolão B. Endocardial and epicardial ablation guided by nonsurgical transthoracic epicardial mapping to treat recurrent ventricular tachycardia. J Cardiovasc Electrophysiol 1998;9:229–239.

Tada H, Nogami A, Naito S, Fukazawa H, Horie Y, Kubota S, Okamoto Y, Hoshizaki H, Oshima S, Taniguchi K. Left ventricular epicardial outflow tract tachycardia: A new distinct subgroup of outflow tract tachycardia. Jpn Circ J 2001;65:723–730.

Uematsu M, Miyatake K, Tanaka N, Matsuda H, Sano A, Yamazaki N, Hirama M, Yamagishi M. Myocardial velocity gradient as a new indicator of regional left ventricular contraction: Detection by a two-dimensional tissue Doppler imaging technique. J Am Coll Cardiol 1995;26:217–223.

Vallès E, Bazan V, Marchlinski FE. ECG criteria to identify epicardial ventricular tachycardia in nonischemic cardiomyopathy. Circ Arrhythm Electrophysiol 2010;3:63–71.

Walker WF, Trahey GE. A fundamental limit on the performance of correlation based phase correction and flow estimation techniques. IEEE Trans Ultrason Ferroelectr Freq Control 1994;41:644–654.